Proceedings of the Korean Nuclear Society Autumn Meeting
Seoul, Korea, October 2001

Thermofluid Dynamics in Molten Reactor Core Pool Surrounded by Crust at High Pressure

J. I. Yun*, K. Y. Suh**, C. S. Kang**

*Future & Challenge Tech. Co.
San 56-1 Sillim-Dong, Kwanak-Gu, Seoul, 151-742, Korea

**Department of Nuclear Engineering, Seoul National University
San 56-1 Sillim-Dong, Kwanak-Gu, Seoul, 151-742, Korea
Phone: +82-2-880-8324, Fax: +82-2-889-2688, E-mail: kysuh@snu.ac.kr

Abstract

Heat transfer and fluid flow in a molten pool are influenced by internal volumetric heat generated from the radioactive decay of fission product species retained in the pool. The pool superheat is determined based on the overall energy balance that equates the heat production rate to the heat loss rate. Decay heat of fission products in the pool was estimated by product of the mass concentration and energy conversion factor of each fission product. For the calculation of heat generation rate in the pool, twenty-nine elements were chosen and classified by their chemical properties. The mass concentration of a fission product is obtained from released fraction and the tabular output of the ORIGEN 2 code. The initial core and pool inventories at each time can also be estimated using ORIGEN 2. The released fraction of each fission product is calculated based on the bubble dynamics and mass transport. Numerical analysis was performed for the TMI-2 accident. The pool is assumed to be a partially filled hemispherical geometry and the change of pool geometry during the numerical calculation was neglected. From the results of numerical calculation, peak temperature of molten pool significantly decreased and volatile fission product was almost released from the molten pool during the accidents.

1. Introduction

A severe accident management concept known as "in-vessel retention" is based on the idea that the vessel lower head will be able to arrest the downward relocation of a degraded core. Lower head integrity can be maintained through the removal process of generated heat. Heat generation in relocated material is mainly caused by radioactive decay of fission products. As the reactor core material melts and relocates, the molten debris pool may be formed in the lower plenum of the reactor pressure vessel or the lower core. If fission product is released from the molten pool, heat source in relocated material may be decreased significantly. Results of the TMI-2 accident analysis [1] indicate that volatile (e.g., I, Cs, Xe) fission products can mostly be released from a molten pool. In the TMI-2 accident, a pool of molten core material was formed and grown within the consolidated region.

The chemical state of the fission products (i.e. vapor pressure) will depend on the temperature and the oxygen potential. During the formation and growth of a pool, the release of volatile fission products would be dominated by bubble dynamics as they all behave as gases. On the other hand the release of non-volatile fission products is controlled by mass transfer because they exist as condensed phases in the pool [2]. The rate of fission product release is calculated using bubble dynamics and mass transfer. For the calculation of heat generation rate in the pool, twenty- nine (29) elements were chosen and classified (see Figure 1). The change of these fission products due to decay chain can be obtained from the tabular output of ORIGEN 2. The multidimensional flow in a molten pool is governed by natural convection with internal heat source [3]. Heat transfer in the pool was treated with the lumped parameter model. The effect of fission product release on pool temperature decrease was estimated with the energy balance. The energy balance, heat transfer and fluid dynamics within the molten pool are described in the next section.

2. Heat Transfer and Fluid Flow

The geometry of a molten pool is assumed to be a partially filled hemisphere. The material is (U, Zr)O_2 with a melting point of ~2850 K. It is assumed that the pool is well mixed. Heat transfer and fluid flow in an oxidic pool shown in Figure 1 are induced by internal volumetric heat generated from the radioactive decay of fission product species retained in the pool. The pattern of flow in the pool having a heat-generating liquid is depicted by natural convection being governed by a Rayleigh number characterizing the relationship between the forces

of buoyancy and viscous friction. If the pool is deep enough, a stable natural-convection current can be formed. Kulacki and Goldstein [4] suggested that convective mixing of the fluid produces a temperature profile that is axially and radially uniform, except for thin laminar boundary layers at the top and at the bottom. Therefore, it is assumed that heat transfer in the pool can be treated with lumped parameter methods without introducing a significant error in the estimation of the pool temperature.

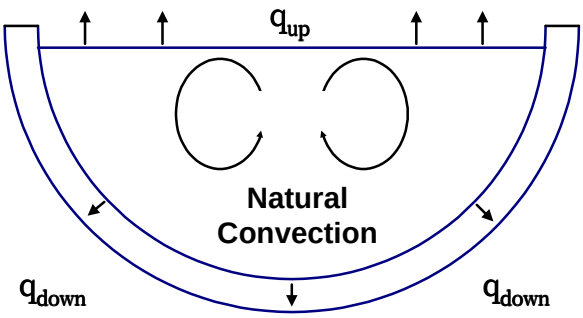

Figure 1: Heat Transfer and Fluid Flow in a Molten Pool

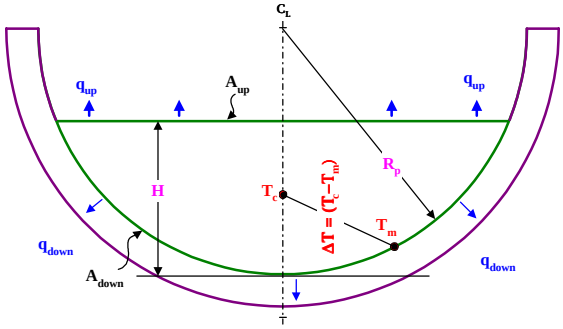

Figure 2: Schematic of the Physical Model

Natural convection phenomena can be scaled in terms of the Grashof (Gr) and Prandtl (Pr) numbers. The presence of volumetric heating necessitates use of the Dammköhler (Da) number. These numbers are expressed [5], respectively, as

$$Gr = \frac{g\beta(T_{\max} - T_i)H^3}{\nu^2},\ \Pr = \frac{\nu}{\alpha},\ Da = \frac{\dot{Q}H^2}{k(T_{\max} - T_i)} \tag{1}$$

The Rayleigh number is given by $Ra = Gr \cdot \Pr \cdot Da$. The behavior of overall heat transfer can be characterized by a correlation in the form of

$$Nu = f(Gr, \Pr, Da) = C_A Ra^{C_B} \tag{2}$$

where C_A and C_B are empirically determined constants, and

$$Ra = \frac{\beta g \dot{Q} H^5}{\nu \alpha k} \tag{3}$$

For the oxidic pool, the ranges of the Ra and Pr numbers are, respectively

$$10^{15} < \mathrm{Ra} < 6\times10^{15} \qquad \Pr \sim 0.6$$

Using the best-known correlations, heat transfer is calculated at the curved bottom and the top of the pool. The correlations are summarized below [6, 7].

$$Nu_{up} = 0.36 Ra^{0.23} \tag{4}$$

$$Nu_{down} = 0.54 Ra^{0.2} (H/R_p)^{0.25} \tag{5}$$

The schematic of the physical model is shown in Figure 2. The overall energy balance that equates the heat production rate to the heat loss rate is

$$V_p \dot{Q} = A_{up} q_{up} + A_{down} q_{down} \tag{6}$$

where A_{up} and A_{down} are surface areas of the partially filled hemispherical geometry in each direction. In the partially filled hemisphere geometry, A_{up} and A_{down} can be determined as follows

$$A_{up} = \pi R_p^2 (1 - x^2) \tag{7}$$

$$A_{down} = 2\pi R_p^2 \cos(\arcsin x) \tag{8}$$

$$x = 1 - H/R_p \tag{9}$$

Substituting equations (4) and (5) into equation (6) to eliminate q_{up} and q_{down}, the pool superheat ΔT may readily be calculated as

$$\Delta T = \frac{H V_p \dot{Q}}{k}[0.54 A_{up} (Ra)^{0.2} (H/R)^{0.25} + 0.36 A_{down} (Ra)^{0.23}] \tag{10}$$

Decrease of decay heat in the pool results from fission product release. Decay heat (i.e. heat source in the pool) of each species equals product of mass and energy conversion factor. Total decay heat in the pool is calculated as:

$$\dot{Q} = \sum_i M_i(t)\eta(i) \tag{11}$$

For twenty-nine (29) elements only, heat generation rate in the pool is calculated. Twenty- nine (29) elements are listed in Table 1. Note that decay power fraction of the remaining elements except the 29 elements are less than 1%. At time t, the initial mass concentration of fission product i in the pool can be obtained by

$$M_{i,0}(t)=[M_{i,j}+(M_{i,j+1}-M_{i,j})\frac{(t-t_j)}{(t_{j+1}-t_j)}](1-f_c)(m_c/m_p) \tag{12}$$

In equation (12), $M_{i,j}$ and t_j can be obtained from the tabular output of the ORIGEN 2 code. Using ORIGEN 2, the initial core and pool inventories at each time can be estimated. With consideration of released fraction of fission product i at time t, the mass concentration of fission product i is estimated as follows

$$M_i(t)=M_{i,0}(t)(1-f_p(t)) \tag{13}$$

Table 1: Radionuclide Elements and Classes

Class	Member Elements
1. Noble gases	Xe, Kr
2. Alkali metals	Cs, Rb
3. Alkaline earths	Ba, Sr
4. Halogens	I, Br
5. Chalcogens	Te, Se
6. Platinoids	Ru, Pd, Rh
7. Transition metals	Mo, Tc, Nb
8. Tetravalents	Ce, Zr, Np
9. Trivalents	La, Pm, Y, Pr, Nd
10. Uranium	U
11. More volatile metals	As, Sb
12. Less volatile metals	Sn, Ag

The thickness of crust surrounding the molten pool can be roughly estimated by considering the steady-state molten pool and crust model illustrated in Figure 3. The mini-ACOPO experiment has shown that the local heat flux varies considerably along the lower boundary of the molten pool [5]. The local heat flux $q_{down}(\theta)$ as a function of annular position from the centerline is presented in Figure 3. From the results of the mini-ACOPO experiment, the local heat flux $q_{down}(\theta)$ is obtained from q_{down} and the shape function as follows

$$\frac{Nu_{down}(\theta)}{Nu_{down}}=0.1+1.08(\frac{\theta}{\varphi})-4.5(\frac{\theta}{\varphi})^2+8.6(\frac{\theta}{\varphi})^3 \qquad \text{when} \quad 0\le\theta/\varphi\le 0.6 \tag{14}$$

$$\frac{Nu_{down}(\theta)}{Nu_{down}}=0.41+0.35(\frac{\theta}{\varphi})+(\frac{\theta}{\varphi})^2 \qquad \text{when} \quad 0.6<\theta/\varphi\le 1.0 \tag{15}$$

In equations (14) and (15) above, φ equals $\cos^{-1}(H/R)$ and means the maximum angle of the molten pool.

The local thickness of the crust $\delta(\theta)$ can be obtained by solving the one-dimensional conduction equation for the crust as

$$\frac{\dot{Q}\delta(\theta)}{2k_{cr}}+\frac{q_{down}(\theta)\delta(\theta)}{k_{cr}}=T_m-T_s(\theta) \tag{16}$$

where k_{cr} is the thermal conductivity of crust. It is assumed that the heat loss from the outer surface of crust is mainly due to thermal radiation unless cooling water enter into the gap between the crust and vessel wall. Therefore, a local energy balance can be given as

$$q_{down}(\theta)+\dot{Q}\delta(\theta)=q_{cr}(\theta)=\varepsilon\sigma T_s{}^4(\theta) \tag{17}$$

where ε is the emissivity of the surface of the crust and σ is the Stenfan-Boltzmann constant. The local thickness of crust can be calculated by combination of equations (14)~(17).

3. Fission Product Release from the Pool

Volatile fission products (Xe, Kr, Cs, I) are insoluble in liquid UO_2. Release of the volatile fission products is dominated by bubble dynamics because they all behave as gases in a molten debris pool. Bubble dynamics in the pool is thus characterized by bubble nucleation, coalescence, growth and rise. The time rate of change for the bubble concentration may be represented as follows (McClure et al. [8])

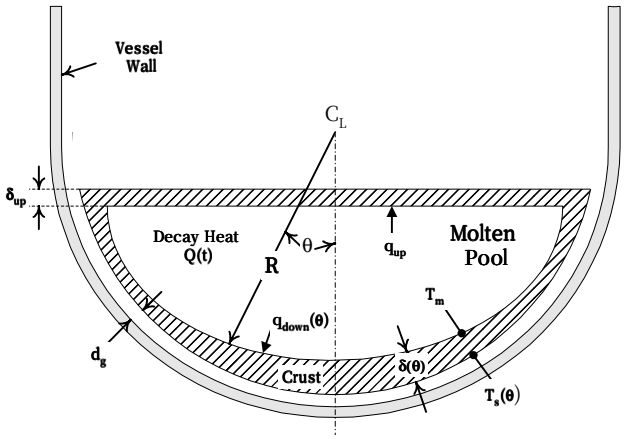

Figure 3: Natural-convection model of the molten pool being surrounded by crust

$$\frac{dn_i}{dt} = \frac{dn_{i,nucl}}{dt} + \frac{dn_{i,coal}}{dt} + \frac{dn_{i,diff}}{dt} - \frac{dn_{i,coal}}{dt} \tag{18}$$

The nucleated bubbles have very small sizes and follow the natural convection flows. Small bubbles coalesce into larger bubbles by turbulence and differential bubble rise in the pool. These bubbles will grow by diffusion of vapor molecules to bubbles. Bubbles can be released from the pool as they sufficiently grow up.

Nucleation of a Bubble

Heterogeneous nucleation of a volatile fission product species will occur when the vapor pressure of the species minus the pool pressure exceeds the surface tension in the bubble-liquid surface:

$$p_g - p_m > (\gamma / R) \tag{19}$$

The number of nucleation sites can be assumed to be proportional to the number of solid particles in the melt. McClure et al. (1993) proposed that the total number of nucleation sites could be represented by summation of temperature-dependent nucleation sites and permanent nucleation sites. The permanent nucleation sites were assumed to exist on temperature-independent surfaces. The number of solid particles in the molten material is assumed to be proportional to the pool mass. The number of sites may be expressed as

$$s_n = (m_p s_{n,t} + s_{n,p}) \tag{20}$$

For small cavity sizes, the bubble size at departure is dictated mainly by a balance between the buoyancy and liquid inertial forces. But, for larger cavity sizes, the bubble size at departure is calculated by a balance of the surface tension and buoyant forces. A well-known equation was proposed by Fritz and Ende (1936) [9] as

$$R_F = 0.0104\theta_0\sqrt{\gamma / g(\rho_l - \rho_v)} \tag{21}$$

This agreed well with the experimental data at atmospheric pressure, but did not concur with the experimental data at super- and subatmospheric pressures. Cole and Shulman (1966) [10] found that, if $R_F = 0.5\sqrt{\gamma / g(\rho_l - \rho_v)}$ for a contact angle of 48°, $\overline{R}_d = R_d / R_F$ is a function of pressure. According to the experimental data, they obtained the following formula

$$\overline{R}_d = \frac{1000}{p} \tag{22}$$

where p is in mm Hg. The nucleation sites emit bubbles with a constant frequency. The frequency can be obtained by the time to grow to the departure diameter by diffusion. The time can be estimated by solving the multi-component diffusion equation. Scriven [11] proposed the following formulation for diffusion of a species to a sphere of changing radius

$$\frac{\partial C}{\partial t} = D\left(\frac{\partial^2 C}{\partial r^2} + \frac{2}{R}\frac{\partial C}{\partial r}\right) - \frac{R^2}{r^2}\frac{dR}{dt}\frac{\partial C}{\partial r} \tag{23}$$

Solution to equation (23) is obtained as (Martins and Szekely [12]) $\varsigma = -a\varphi(\beta_b)$

where

$$\varphi(\beta_b) = 2\beta_b{}^3 \exp(3\beta_b{}^2) \times \int_S^\infty \xi^{-2} \exp(-\xi^2 - 2\beta_b{}^3\xi^{-1}) d\xi \tag{24}$$

$$\zeta = \frac{C - C_m}{C_m} \quad \text{and} \quad a = D\frac{A}{C_m} \tag{25}$$

The growth constant β_b can be obtained from Scriven's useful expression of solutions to equation (23)

$$\varphi(\beta_b) \sim \sqrt{(\pi/3)}[\beta_b - 4/9 + 0(\beta_b^{-1})] \tag{26}$$

Data of Scriven's tabulation are incorrect for especially small values of $\varphi(\beta_b)$. This error is induced through the change of variable in integral equation . In this study, new tabulation is obtained, as shown in Figure 4 and 5, by numerical integration of equation (24) using the Simpson's method. The results show that values of β_b for small $\varphi(\beta_b)$ are much smaller than those of Scriven's tabulation, and values of β_b for large $\varphi(\beta_b)$ are close to half values of his tabulation.

Once β_b is known, the bubble detachment frequency can be calculated as

$$f_d = \frac{1}{t} = \frac{4\beta_b{}^2 D}{R^2} \tag{27}$$

The product of the bubble detachment frequency and the number of nucleation sites determines the rate at which bubbles are formed, viz.

$$\frac{dn_{i,nucl}}{dt} = f_d \cdot s_n \tag{28}$$

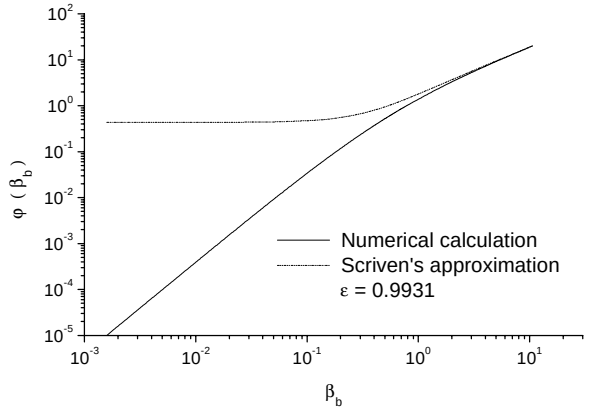

Figure 4: The variation of $\varphi(\beta_b)$ for small value of β_b

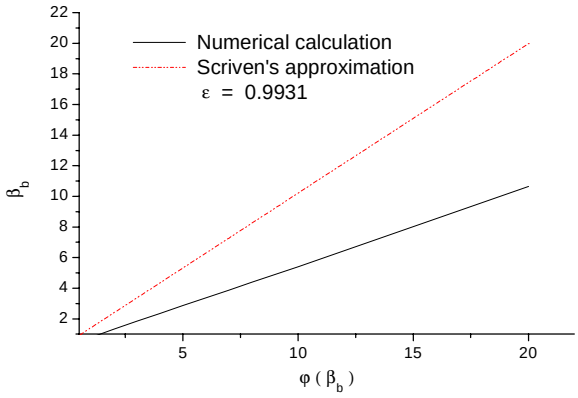

Figure 5: The numerical results of β_b for large values of $\varphi(\beta_b)$

Diffusion to a Bubble

Diffusion to a bubble is governed by equation (23) used to calculate nucleation rate of the bubble. The rate of change of number density for bubble size R_i can be determined by the time to grow from bubble size R_{i-1} to size R_i. The rate of change of a discrete bubble radius R_i is the sum of loss term and production term. The loss term equals the number density of bubbles of size R_i divided by the time to grow from size R_i to size R_{i+1} and the production term is the number density of bubbles of size R_{i-1} divided by the time to grow from size R_{i-1} to size R_i. Therefore, the rate of change of number density for bubble size R_i is represented as

$$\frac{dn_{i,diff}}{dt} = \frac{n_{i-1}}{t_i - t_{i-1}} - \frac{n_i}{t_{i+1} - t_i} \tag{29}$$

Coalescence of Bubbles

Bubbles interact due to their motion and grow by coalescence. The rate of coalescence of a bubble of radius R_k is given by Olander [13] as

$$dn_k / dt = 0.5 \sum_{i+j=k} B_{ij} n_i n_j - \sum_{i=1} B_{ik} n_i n_k \tag{30}$$

The rate of change of number density for bubble size R_k can also be obtained by summation of production term and loss term. The production term is represented by the rate of formation of bubble size R_k due to collisions of bubbles of sizes R_i and R_j. The loss term is represented by the rate of disappearance of bubble size R_k due to coalescence with bubbles of other sizes. It is assumed that bubble coalescence is caused by two mechanisms, i.e. turbulence in the pool and differential rise velocity of bubbles. For the turbulence process, a correlation for aerosol agglomeration in turbulent pipe flow is used as presented by Friedlander [14]

$$B_{ij,turb} = 1.3(R_i + R_j)^3 (\varepsilon_d / \nu)^{1/2} \tag{31}$$

where

$$\varepsilon_d / \nu = (2/R_p)(f/2)^{1.5} v_{conv}^3 \tag{32}$$

The convective velocity in the pool can be obtained from an energy balance and is given by

$$v_{conv} = 2Q/(\rho A_{conv} c_p \Delta T) \tag{33}$$

For coalescence due to differential bubble rise velocity, the frequency function is also given by Friedlander [14] as

$$B_{ij,rise} = \pi (R_i + R_j)^2 \left| v_i - v_j \right| \tag{34}$$

For all the fission product release calculations, the molten pool is assumed to be a partially filled hemisphere. The material is (U, Zr)O_2 with a melting point of ~2850 K. It is assumed that the pool is homogeneous.

Loss of Bubbles due to Bubble Rise

The rate at which bubbles leave the pool is proportional to the bubble number density and the rise velocity. The residence time of bubbles of size R_k is given by the pool height divided by the rise velocity. It is assumed that the rate at which bubbles leave the pool equals the number density of bubbles divided by the residence time in the pool. The rise velocity of a spherical gas bubble is found by balancing the drag and buoyant forces on the bubble. Hence,

$$v = 2\rho g R^2 / 9\mu \tag{35}$$

The rate of the loss of bubbles due to buoyant rise can be calculated by:

$$\frac{dn_{i,loss}}{dt} = \frac{v_i n_i}{z} \tag{36}$$

Fission Product Release through Mass Transport

The less volatile fission products tend to remain as condensed phases in the melt because of their low vapor pressures. The chemical forms of the less volatile fission products in the melt are determined by the oxygen potential. It is assumed that mass transport governs release of the less volatile fission product from the pool. At high temperature (>2850 K), rare earth elements such as europium and cerium exist as oxides, strontium is present as SrO, and ruthenium and antimony are present as metals immiscible in the molten pool (Petti, et al. [15]). The rate of mass transport of a species in a liquid is given by

$$\dot{m} = k_m A_{up} (C_\infty - C_{surf}) \tag{37}$$

The mass transfer correlations for the top of the pool can be obtained by means of a heat and mass transfer analogy

Table 2: Values and Ranges of Parameters

Parameter	Value
Pool mass , M_p [kg]	32,700
Pool radius, R_p [m]	1.45
Pool pressure, p [MPa]	0.1 ~ 10.0
Pool velocity, V_{conv} [m/sec]	0.13
Number of permanent nucleation sites [site/kg]	100 ~ 1000
Number of temperature-dependent nucleation sites [site/kg]	100 ~ 30,000
Diffusivity of fission product [m^2/sec]	1×10^{-11} ~ 1×10^{-7}
Surface tension of liquid in pool γ [N/m]	0.5 ~ 1.6

4. Results and Discussion

For all the fission product release calculations in this work, the main parameters were obtained from the analysis report of the TMI-2 accident (Akers, et al. [1]). The pool is assumed to be a partially filled hemisphere,

1.45 m in radius and 32,700 kg in mass. The change of pool geometry during the numerical calculation is neglected. The fission product inventories in the pool are about 24.5% of the total core inventories. The parameters used in the numerical calculations are listed in Table 2. From the numerical analysis, the height of the pool is 1.014 m and peak temperature at the pool center exceeds 3000 K.

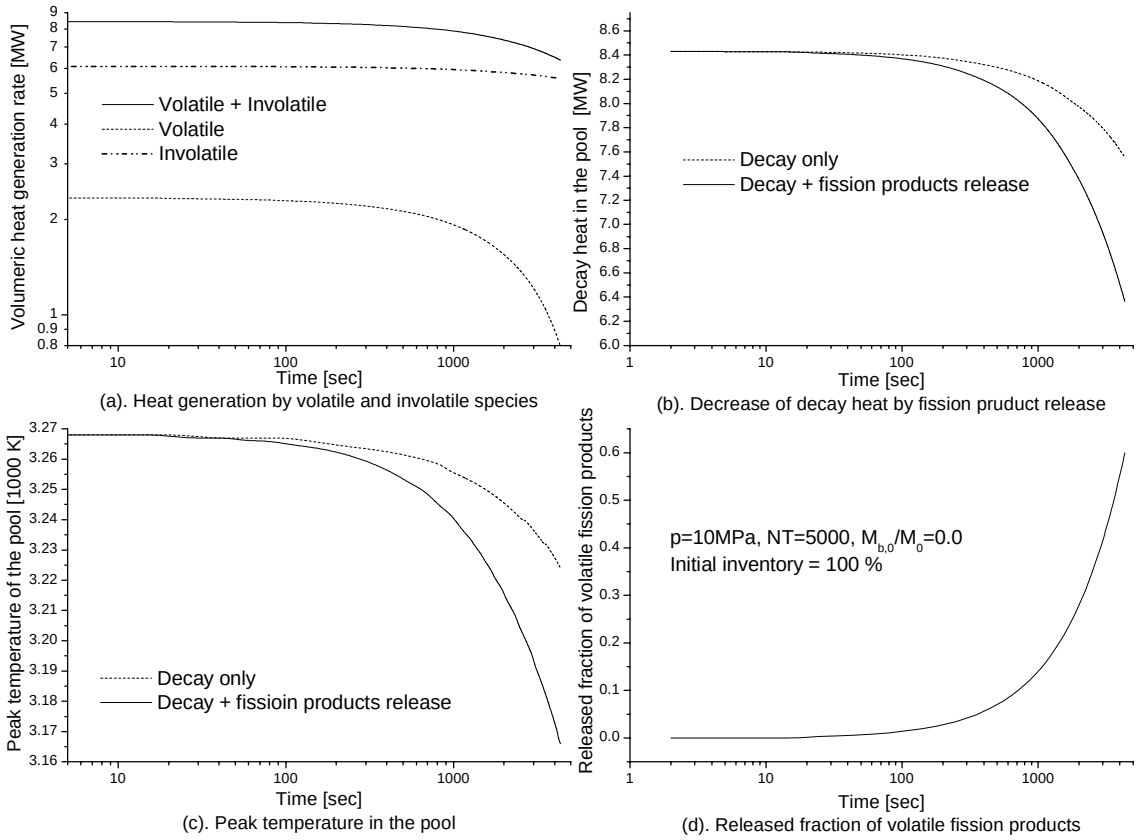

Figure 6: Heat generation and transfer in case of mass ratio ($M_{b,0}/M_0$) = 0.0

The calculations were carried out with p=10 MPa, ns_t=5000, and initial inventory = 100 %. In each cases of $M_{b,0}/M_0$=0 and 0.5, times to release 60 % of volatile gas inventory are about 4350 and 750 sec as shown in Figure 6-(d) and 7-(d). From concentrations of the 29 elements in the pool, total heat generation rate was obtained at time t. Figure 6-(a) and 7-(a) comparatively show the difference of volumetric heat generation rate between the volatile and non-volatile fission products. Figure 6-(b) and (c) show decrease of decay heat by fission product release and the peak temperature in the pool. When release of the fission products from the debris pool is considered, the peak temperature of the pool decreases from 3224 K to 3166 K at 4346 sec as shown in Figure 6-(c). In Figure 7-(c), also, the peak temperature in the pool decreases from 3260 K to 3194 K at 745.5 sec. Because Initial bubbles interact and rapidly grow by coalescence and diffusion to a bubble, if bubbles in molten core material exist before the formation of the pool, pool peak temperature decreases faster.

When thermal properties of the pool are taken to be: $k = 4\ W/mK$, $\alpha = 9.1 \times 10^{-7}\ m^2/s$, $\nu = 5.9 \times 10^{-7}\ m^2/s$, and $\beta = 9.1 \times 10^{-7}\ K^{-1}$. Pool Rayleigh number is about $3 \sim 3.5 \times 10^{15}$. Table 3 shows pool specific heat and average downward heat flux at the time to release 60% of volatile gas inventory. Under the condition which fission products release, pool specific heat and average downward heat flux are significantly reduced by removal mechanism of heat source. Therefore, fission product release may be considered to best estimate heat source of the pool and lower head integrity.

5. Conclusions

When fission products release from the molten pool, heat source of the pool was estimated using 29 nuclides concentration data of ORIGEN 2 code and heat flux, pool specific heat and peak temperature were calculated by overall energy balance. The heat generation rate decreases faster, if initial bubbles exist in the pool, because of release of mainly volatile fission gas. The peak temperature sizably decreased by about 60 K as the fission products are released from the pool. For both cases with $M_{b,0}/M_0$ = 0.0 and 0.5, heat flux is reduced by ~20%.

From results of numerical analysis, it is concluded that fission product release may be considered to best estimate heat source of the pool and lower head integrity

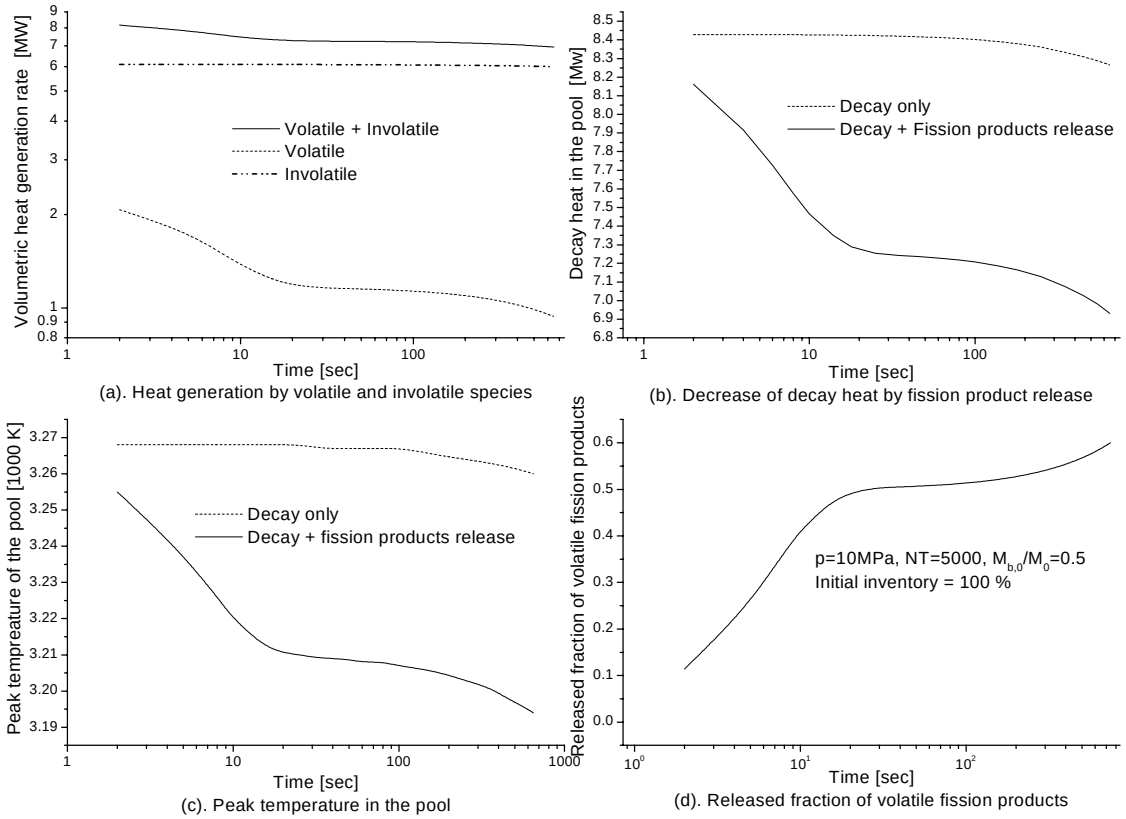

Figure 7: Heat generation and transfer in case of mass ratio ($M_{b,0}/M_0$) = 0.5

Table 3: Pool specific heat and heat flux of the pool

Mass ratio	Release	Decay heat rate, $\dot{Q}$	Pool specific heat, ΔT	Heat flux, q_{down}
0.0	No	7.55	374.5	9.34E5
	Yes	6.37	315.6	7.61E5
0.5	No	8.27	409.8	1.04E6
	Yes	6.93	343.7	8.42E5

Nomenclature

A	area of bubble surface (m^2)
A_{conv}	area for convection (m^2)
A_{down}	area for downward heat transfer (m^2)
A_{up}	area for upward heat transfer (m^2)
B	coalescence frequency function (m^3/s)
C	fission product concentration in the pool ($No./m^3$)
c_p	specific heat capacity (J/kgK)
f	Fanning friction factor (0.004)
$f_{c,i}$	released fraction of species i before formation of the pool

f_p released fraction of species i from the pool
H depth of the pool (m)
k thermal conductivity ($W/m \cdot K$)
k_m mass transfer coefficient (m/s)
$\dot{m}$ rate of mass transport (kg/s)
m_c mass of the core (kg)
m_p mass of the pool (kg)
$M_{b,0}$ mass of volatile species in the initial bubbles (kg)
$M_{i,0}$ initial inventory of volatile fission product i in the pool (kg)
M_0 initial inventory of volatile species in the pool ($= \sum_i M_{i,0}$) (kg)
n number density of bubble ($No./m^3$)
ns_p number of permanent nucleation sites ($No.$)
ns_t number density of temperature-dependent nucleation sites ($No./kg$)
$\dot{Q}$ volumetric heat generation rate (W/m^3)
p pressure of the pool (N/m^2)
p_g pressure of gas bubble (N/m^2)
q average heat flux over a boundary (W/m^2)
R radius of bubble (m)
R_d radius of bubble at departure (m)
R_P radius of the molten pool (m)
T temperature of the pool (K)
ΔT superheat of the pool (K)
V_P volume of the pool (m^3)
v velocity of bubble (m/s)

Greek Letters

α thermal diffusivity (m^2/s)
β thermal expansion coefficient (K^{-1})
β_b growth constant of diffusion to a bubble
γ bubble-melt interfacial tension (N/m)
η heat generation per unit mass (W/kg)
ε Stefan-Boltzmann constant (5.6E10-8) (W/m^2K^{-4})
ε_d eddy diffusivity (m^2/s^3)
κ gas constant (Boltzmann constant) (J/K)
θ_0 contact angle of nucleating bubble (°)
ν kinematic viscosity ($kg/m \cdot s$)
ρ_m density of the pool (kg/m^3)
μ viscosity of the pool ($N \cdot s/m^2$)

Subscripts

0 initial value or nominal value
∞ value in the bulk
coal coalescence
conv convection
diff diffusion
nucl nucleation
loss loss due to bubble rise
surf surface

References

[1] Akers, D.C., et al., "Three Mile Island Unit 2 Fission Product Inventory Estimates," Nuclear Technology, Vol. 87, pp 205-213, 1989.

[2] Iglesias, F.C., et al., "Fission Product release Mecha-nisms during Reactor Accident Conditions," Journal of Nuclear Materials, Vol. 270, pp 21-38, 1999.

[3] "Behavior of Corium Melt Pool Under External Cooli-ng," Final Report of the First Phase of RASPLAV Project, Kurchatov Institute, Russia, January 1988.

[4] Kulacki, F. A. and Goldstein, R. J., "Thermal Convec-tion in a Horizontal Fluid Layer with Uniform Volumetric Energy Sources," J. Fluid Mech., Vol. 55, Part 2, p 271, 1972.

[5] Theofanous, T.G., et al., "In-Vessel Coolability and Retention of A Core Melt," DOE/ID-10460, 1994.

[6] Asfia, F. J., Frantz, B. and Dhir, V. K., "Experimental Investigation of Natural Convection in Volumetrically Heated Spherical Segments," Submitted for Publication in J. of Heat Transfer, 1994.

[7] Mayinger, F., et al. "Examination of Thermohydraulic Processes and Heat Transfer in a Core Melt," Final Report BMFT RS 48/1, Hannover Technical University, Germany, 1975.

[8] McClure, P.R., Leonard, M. T. and Razani, A., "A Model for Fission Product Release from Liquid-Metal Pools: Development and Sensitivity Investigation," Nuclear Science and Eng., Vol. 114, pp. 102-111, 1993.

[9] Fritz, W. and Ende, W., "Uber den Verdampfungsvor-gang nach Kinematographischen Aufnahmen an Dampfbla-sen," Physik Zeitscher, Vol.37, pp. 391-401, 1936.

[10] Cole, R. and Shulman, H.L., "Bubble Departure Dia-meters at Subatmospheric Pressures," Chemical Engineers Progress Symposium Series 62, Vol. 64, pp. 6-16, 1966.

[11] Scriven, L.E., "On the Dynamics of Phase Growth," Chem. Eng. Sci., Vol. 10, pp. 1-13, 1959.

[12] Martins, G.P. and Szekely, J., "On Spherical Phase Growth in Multicomponent Systems," Transactions of the Metallurgical Society of AIME, Vol. 245, pp. 1741-1747, August 1969.

[13] Olander, D. R., "Fundamental Aspects of Nuclear Reactor Fuel Elements," TID-26711-P1, Department of Energy, Washington, DC, USA, 1976.

[14] Friedlander, S.K., "Smoke, Dust and Haze: Funda-mentals of Aerosol Behavior," John Wiley and Sons, New York, NY, USA, 1977.

[15] Petti, D. A., et al., "Analysis of Fission Product Release Behavior from the Three Mile Island Unit 2 Core," Nuclear Technology, Vol. 87, p 243-263, August 1989.